

NONUNIFORMLY SAMPLED TRIVARIATE EMPIRICAL MODE DECOMPOSITION

Apit Hemakom^{1*} Alireza Ahrabian¹ David Looney¹ Naveed ur Rehman² and Danilo P. Mandic¹

¹ Imperial College London

² COMSATS Institute of Information Technology
{apit.hemakom12, d.mandic}@imperial.ac.uk

ABSTRACT

Multichannel data-driven time-frequency algorithms, such as the multivariate empirical mode decomposition (MEMD), have emerged as important tools in the analysis of inter-channel dependencies that arise in multivariate data. Such methods employ uniform projection schemes on hyperspheres in order to estimate the local mean, thus requiring dense but underutilised sampling when processing unbalanced data channels. To this end, we propose a nonuniform projection scheme that adapts to the second order statistics of trivariate data; this provides the estimation of the local mean in the case of power imbalances and correlations between the channels. The algorithm is particularly useful for generating a low number of direction vectors within MEMD. Its performance is illustrated on synthetic and real-world data.

Index Terms— Trivariate EMD, non-uniform sampling, Hilbert transform, multiscale processing.

1. INTRODUCTION

Empirical mode decomposition (EMD) is a signal decomposition algorithm that was developed for the analysis of non-linear and non-stationary data [1]. The algorithm adaptively identifies a set of basis functions from the signal, termed intrinsic mode functions (IMFs), using a sifting process. The IMFs are narrow-band amplitude/frequency-modulated (AM/FM) components and, via the Hilbert transform, admit a highly localised time-frequency representation [2, 3]. Compared to conventional projection-based time-frequency methods such as the short-time Fourier transform, the data-driven nature of the EMD has enabled more physically meaningful analysis in applications ranging from bio-signal processing [4, 5] and oceanography [6] to palaeoclimatology [7].

An implication of the empirical nature of standard EMD is that its application to multichannel data typically results in IMFs with differing oscillatory dynamics across data channels for a given IMF index. Furthermore, similar oscillatory modes may appear across multiple IMFs, obscuring multichannel data analysis based on the univariate EMD [8]. To

this end, several extensions of EMD have been proposed, namely complex EMD (CEMD) [9], rotation-invariant EMD (RIEMD) [10], bivariate EMD (BEMD) [11], trivariate EMD [12] and multivariate EMD (MEMD) [13, 14]. Applications of MEMD include feature estimation [15] and artifact removal [16, 17].

It should be noted that as EMD-based algorithms perform signal decomposition based on the identification of a set of adaptive basis functions of a signal, a mathematical description of these techniques is still lacking. To this end, the work in [18] proposed an alternative approach to EMD called the synchrosqueezing transform (SST). This method reallocates the energies of resulting wavelet coefficients generated by the continuous wavelet transform (CWT) by combining the coefficients containing the same instantaneous frequency, resulting in a highly localised time-frequency representation of a univariate signal. More recently a multivariate extension of the SST [19] has been proposed to identify a set of modulated oscillatory components common to the multivariate data. Applications include multivariate time-frequency analysis [19] and multivariate signal denoising [20], whereby inter-channel dependencies are employed for enhanced signal analysis.

The sifting algorithm employed in both the BEMD and MEMD projects the multichannel input signal along multiple uniformly-sampled direction vectors in multidimensional space so as to estimate the local mean. However, as real-world signals often contain power imbalances or inter-channel correlations, these vectors may not best represent the inter-channel dependencies of multichannel data, resulting in the sub-optimal estimation of the local mean. To this end, the work in [21] introduced the nonuniformly sampled BEMD (NS-BEMD), which exploits the second-order statistics of bivariate signals, namely inter-channel correlations and power discrepancies between data channels, yielding a global set of projections which map the signal to the direction of highest curvature. The work in [22] introduced dynamically-sampled BEMD (DS-BEMD), an adaptive projection scheme based on the local signal dynamics. The DS-BEMD quantifies local signal dynamics via Menger curvature, so as to generate projection vectors according to the directions in 2-dimensional space where the signal exhibits highest local dynamics.

Both extensions of NS- and DS-BEMD algorithms to

*Thanks to the Royal Thai Government for funding.

the multivariate case (greater than 2 channels) were/are open problems for which a potential solution has been proposed for the NS-BEMD algorithm. This work extends the bivariate case to introduce a nonuniformly sampled trivariate EMD (NS-TEMD). This is achieved based on global nonuniform sampling first introduced in [21], so as to identify direction vectors that adapt to the second order statistics of trivariate data.

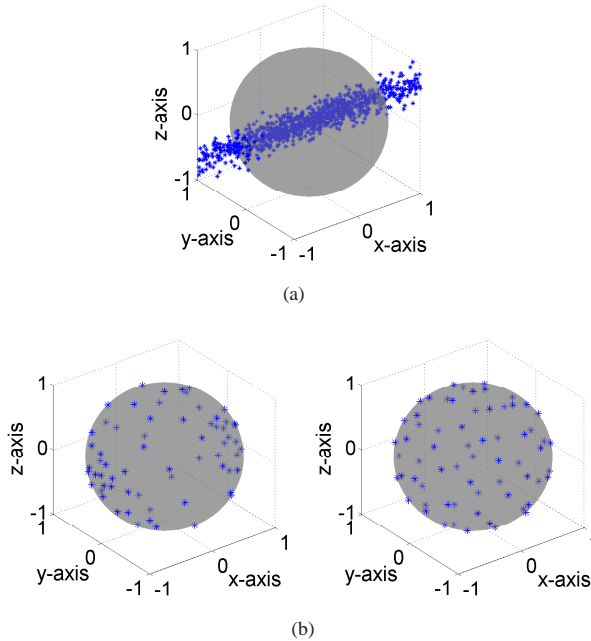


Fig. 1. TEMD sampling for unbalanced data. (a) The scatter plot of a three-channel data source, exhibiting a significant power imbalance. (b) The proposed sampling scheme (left panel) for the three-channel data source shown in (a). The corresponding uniform sampling scheme employed for the TEMD (right panel).

2. NONUNIFORMLY SAMPLED TRIVARIATE EMD

The NS-BEMD algorithm in [21] enhanced the performance of the conventional BEMD for bivariate data with non-circular statistics. This was achieved by relating the second order statistical structure of the bivariate data, captured by the circularity quotient, to the parameters of an ellipse; such that the resulting samples were localised along the directions of principal importance. A detailed explanation of the NS-BEMD can be found in [21].

In the case of trivariate signals, identifying the directions of highest curvature in three dimensional space is a non-trivial task. This is particularly the case when attempting to identify a set of global nonuniformly sampled projections, as the nonuniform samples may not align with the directions

of highest curvature within trivariate/multivariate signals, resulting in a suboptimal estimate of the local mean. In order to overcome this problem, a combination of uniform sampling of the sphere along with a nonuniform sampling scheme is proposed. By employing uniform samples, the directions of highest curvature not captured by the nonuniform samples are also used for projecting the input signal, yielding a more accurate estimate of the local mean.

In order to develop a ‘global’ nonuniform sampling scheme for the trivariate and ultimately multivariate EMD, the directions of principal importance need to be determined. As with the NS-BEMD, the directions of principal importance are defined in terms of inter-channel power imbalances and correlations. For a given multivariate signal, $\mathbf{x}(t)$, with a covariance matrix given by $\mathbf{C} = E\{\mathbf{x}^T(t)\mathbf{x}(t)\}$ (where $E\{\cdot\}$ is the statistical expectation operator and $(\cdot)^T$ is the transpose operator), the directions of principal importance can then be determined by carrying out an eigendecomposition of the covariance matrix, $\mathbf{C} = \mathbf{V}\mathbf{\Lambda}\mathbf{V}^T$, where the entries of a diagonal matrix $\mathbf{\Lambda}$ correspond to the eigenvalues and the matrix \mathbf{V} corresponds to the eigenvectors of the covariance matrix \mathbf{C} . The eigenvector matrix, \mathbf{V} , captures the directions of principal importance of a given trivariate signal, while the eigenvalues determine the relative power of the resulting directions.

In order to generate nonuniform samples based on the statistical structure of the input trivariate signal, an ellipsoid with the following Cartesian coordinates ($x - y - z$ axis) is generated

$$\begin{aligned} x &= a \cos \theta \sin \phi \\ y &= b \sin \theta \cos \phi \\ z &= c \cos \phi \end{aligned} \quad (1)$$

where θ is the inclination angle, ϕ corresponds to the azimuth angle, and the terms a, b, c are parameters used to determine the ellipsoid in three dimensional space. The inclination and azimuth angles correspond to the directions of a uniformly sampled sphere (Hammersley sequence [13]), such that the resulting ellipsoidally distributed samples are located along the directions of highest curvature.

Algorithm 1: Nonuniformly sampled Trivariate EMD (NS-TEMD)

1. Given a trivariate signal $\mathbf{x}(t)$, perform the eigendecomposition of the covariance, $E\{\mathbf{x}\mathbf{x}^T\} = \mathbf{V}\mathbf{\Lambda}\mathbf{V}^T$, where \mathbf{V} is the eigenvector matrix, and $\mathbf{\Lambda} = \text{diag}\{\lambda_1, \lambda_2, \lambda_3\}$, is the eigenvalue matrix, with the eigenvalues, $\lambda_1 > \lambda_2 > \lambda_3$.
2. Uniformly sample a sphere using the Hammersley sequence, and determine the corresponding azimuth angle ϕ_H , and inclination angle θ_H of the Hammersley projections, in order to identify the Cartesian coordinates of the uniformly sampled sphere.

3. Determine the nonuniform projection $\hat{\mathbf{e}}_p$ on a sphere by constructing an ellipsoid with the following parameters

$$\hat{\mathbf{e}}_l = \begin{bmatrix} \lambda_1^{\frac{1}{3}} \cos \theta_H \sin \phi_H \\ \lambda_2^{\frac{1}{3}} \sin \theta_H \cos \phi_H \\ \lambda_3^{\frac{1}{3}} \cos \phi_H \end{bmatrix} \quad (2)$$

Rotate the ellipsoid, $\hat{\mathbf{e}}_l$, such that the directions of highest curvature are sampled, $\hat{\mathbf{e}}_p = \mathbf{V}\hat{\mathbf{e}}_l$.

4. Perform the local mean estimation according to the conventional MEMD algorithm (see [13] for more details), using both the uniform samples and the nonuniform samples $\hat{\mathbf{e}}_p$.

3. SIMULATION RESULTS

The performance of the NS-TEMD algorithm was evaluated over simulations on trivariate signals with varying channel powers, and on noise assisted signal decomposition on synthetic data and an event-related potential (ERP) signal from the electroencephalography (EEG). All the simulations employed 32 projection vectors, as 16 projection vectors are inadequate to capture the direction of highest curvature of trivariate signals, and employing a larger number of projection vectors is computationally intensive.

3.1. Bivariate Data with Varying Channel Powers

We next examined the performance of the proposed NS-TEMD algorithm in denoising a three channel signal consisting of sinusoidal oscillations, and against those of MEMD and multivariate wavelet synchrosqueezing denoising (MWSD) algorithm [20]. The SNR of the first channel was varied between 17 dB and -1 dB, while the SNR of the second and

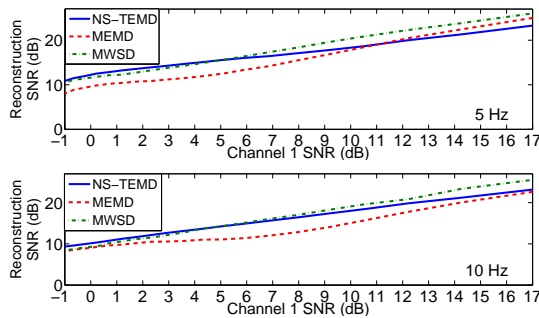


Fig. 2. Reconstruction error (in SNR) for the IMFs of a sinusoid (upper panel: 5Hz, lower panel: 10Hz) using the proposed NS-TEMD, MEMD and MWSD algorithms.

third channel were fixed at 30 dB; the corresponding reconstruction SNR of the sinusoid in the first channel was then calculated for a given IMF index.

Fig. 2 shows the reconstruction SNR for the proposed algorithm against the MEMD and the MWSD, when processing sinusoidal oscillations with frequencies of 5 Hz and 10 Hz. It can be observed that the proposed method outperforms the MEMD in recovering the 10 Hz sinusoid with approximately 3dB of improvement when there exists a power imbalance between channel 1 with respect to the second and third channels of approximately 18-27 dB (the SNR of the first channel was 3-12 dB). For the 5 Hz sinusoidal oscillation the reconstruction SNR of NS-TEMD was approximately 3dB higher than that of MEMD, when there exists a significant power imbalance between the relevant channels. The proposed algorithm, however, performs similar to MWSD in recovering the 5 Hz and 10 Hz sinusoidal signals when the power imbalance was relatively low (lower than 4 dB).

3.2. Noise Assisted Signal Decomposition

In this section the performance of the proposed nonuniformly sampled TEMD algorithm was assessed against the MEMD (using only three channels) for a noise-assisted decomposition of a two tone sinusoidal oscillation. For this simulation the first channel consisted of a discrete time signal (sampled at $f_s = 1000$ Hz), given by

$$x^1 = \cos 2\pi \frac{10}{f_s} n + \cos 2\pi \frac{15}{f_s} n, \quad (3)$$

and the second and third channels were WGN processes. The relative power of the second and third channel was constant, while the SNR of the first channel relative to noise channels

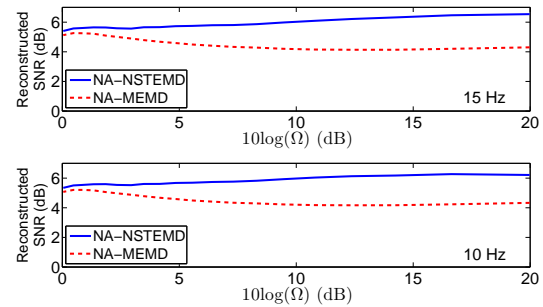


Fig. 3. Reconstruction error (in SNR) for the IMFs for a two-tone signal in (3) with varying channel power ratio, given by $10 \log(\Omega)$, with $\Omega = \frac{\text{Signal power}}{\text{Noise channel power}}$. (upper panel) Reconstruction of both the NA-NSTEMD and NA-MEMD algorithm for the 15 Hz tone. (lower panel) Reconstruction of both the NA-NSTEMD and NA-MEMD algorithm for the 10 Hz tone.

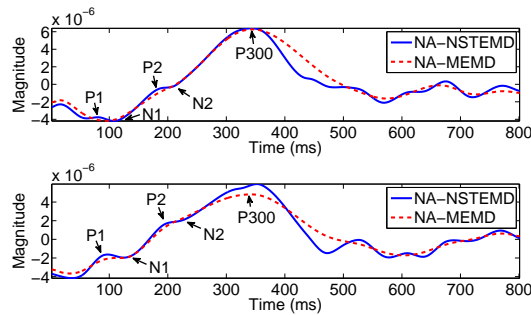


Fig. 4. ERP ground truth generated by performing MEMD and NS-STEMD on EEG data recorded from the Fz electrode (upper panel) and Cz electrode (lower panel) during an ERP experiment.

was varied from 0 dB to 20 dB. Fig. 3 shows the reconstructed SNRs for both the proposed noise-assisted NS-STEMD (NA-NSTEMD) and noise assisted MEMD (NA-MEMD, see [23] for more details) algorithms; the reconstruction SNR for the proposed method improved as the relative SNR increased, while for the NA-MEMD the performance decreased with the degree of a power imbalance between the data channels.

3.3. ERP component decomposition

Event-related potentials are elicited sensory responses of the brain, generated primarily from auditory and/or visual stimuli and measured via EEG [24]. Major ERP components include the P1, N1, P2, N2 and P300. The P300 can be elicited through unexpected stimuli. The subject was shown randomly coloured boxes (non-target stimuli) and a box with white background and red foreground (target stimulus); both types of stimuli were generated using an LCD screen. The time intervals between each of the desired stimuli were randomised. The ERP signals were band-pass filtered to 1-20 Hz and averaged over 10 trials. A multichannel signal was then constructed from ERP data recorded from the Fz and Cz electrodes forming the first and second channels, while the third channel for both algorithms contained white Gaussian noise to enforce a dyadic filterbank structure within the EEG channels and enable noise-assisted mode-of-operation in both algorithms. Fig. 4 shows the ground truth of the ERP data generated by averaging 1000 ERP-IMFs obtained from applying 1000 realisations of the NA-NSTEMD and NA-MEMD on the multichannel signal. In order to evaluate the performance of both the NA-MEMD and NA-NSTEMD algorithms, the mean squared error (MSE) for each realisation of the estimated ERPs was calculated with respect to the ground truth ERPs for each electrode.

Observe from Fig. 5 that the NA-NSTEMD yielded significantly lower MSE compared to NA-MEMD for ERP sig-

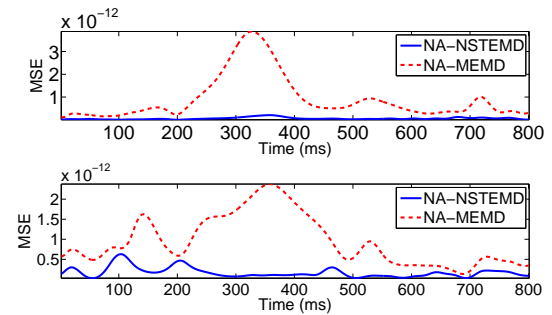


Fig. 5. Mean squared error of ERP components at the Fz electrode (upper panel) and Cz electrode (lower panel).

nals from both the Fz and Cz electrodes, and the MSE for the NA-MEMD approach was particularly high during the P300 which, in BCI applications, is the most important component of the ERP.

Observe from Table 1 that the NA-NSTEMD outperformed the NA-MEMD. The case when the NA-NSTEMD was used to decompose a single channel of an ERP signal from either the Fz or Cz electrode with the other two channels being WGN did not outperform the NA-MEMD (the result is not shown). This is because there was no inter-channel dependency or imbalance which is essential in generating nonuniformly sampled projection vectors in NS-STEMD.

Table 1. The average MSE along time of the NA-NSTEMD and NA-MEMD algorithms from the Fz and Cz electrodes.

	Fz	Cz
NA-NSTEMD	5.35×10^{-14}	1.67×10^{-13}
NA-MEMD	1.00×10^{-12}	9.36×10^{-13}

4. CONCLUSION

A NS-STEMD algorithm has been introduced in order to generate projection vectors that represent the principal direction in three dimensional space for unbalanced trivariate signals. The proposed algorithm has been shown to outperform conventional MEMD in decomposing trivariate noisy signals with modest SNRs and outperformed the MWSD when SNRs were low. In the presence of white Gaussian noise, the proposed algorithm has been shown to be more effective than NA-MEMD. Simulations on both synthetic and EEG data support the analysis; NA-NSTEMD yielded significantly lower MSE in decomposing ERP components compared to NA-MEMD, showing its potential to recover responses in real-world data.

5. REFERENCES

- [1] N.E. Huang, Z. Shen, S.R. Long, M.C. Wu, H.H. Shih, Q. Zheng, N. Yen, C.C. Tung, and H.H. Liu, "The empirical mode decomposition and the Hilbert spectrum for nonlinear and non-stationary time series analysis," *Proceedings of the Royal Society A*, vol. 454, pp. 903–994, 1998.
- [2] N.E. Huang, M.C. Wu, S.R. Long, S.S.P. Shen, W. Qu, P. Gloersen, and K.L. Fan, "A confidence limit for the empirical mode decomposition and Hilbert spectral analysis," *Proceedings of the Royal Society A*, vol. 459, pp. 2317–2345, 2003.
- [3] L. Cohen, *Time-Frequency Analysis*, Prentice-Hall, 1995.
- [4] T.M. Rutkowski, D.P. Mandic, A. Cichocki, and A.W. Przybyszekski, "EMD approach to multichannel EEG data – the amplitude and phase components clustering analysis," *Journal of Circuits, Systems, and Computers*, vol. 19, no. 1, pp. 215–229, 2010.
- [5] E.P.S. Neto, P. Abry, P. Loiseau, J.C. Cejka, M.A. Cus-taud, J. Frutoso, C. Gharib, and P. Flandrin, "Empirical mode decomposition to assess cardiovascular autonomic control in rats," *Fundamental and Clinical Pharmacology*, vol. 21, pp. 481–496, 2007.
- [6] X. Chen, Y. Zhang, M. Zhang, Y. Feng, Z. Wu, F. Qiao, and N.E. Huang, "Intercomparison between observed and simulated variability in global ocean heat content using empirical mode decomposition, part i: modulated annual cycle," *Climate Dynamics*, vol. 41, pp. 2797–2815, 2013.
- [7] X. Chen, Z. Wu, and N.E. Huang, "The time-dependent intrinsic correlation based on the empirical mode decomposition," *Advances in Adaptive Data Analysis*, vol. 2, no. 2, pp. 233–265, 2010.
- [8] D. Looney and D.P. Mandic, "Multiscale image fusion using complex extensions of EMD," *IEEE Transactions on Signal Processing*, vol. 57, no. 4, pp. 1626–1630, 2009.
- [9] T. Tanaka and D.P. Mandic, "Complex empirical mode decomposition," *IEEE Signal Processing Letters*, vol. 14, no. 2, pp. 101–104, 2007.
- [10] M.U. Altaf, T. Gautama, T. Tanaka, and D.P. Mandic, "Rotation invariant complex empirical mode decomposition," *Proc. of IEEE International Conference on Acoustics, Speech and Signal Processing*, vol. 3, pp. 1009–1112, 2007.
- [11] G. Rilling, P. Flandrin, P. Goncalves, and J.M. Lilly, "Bivariate empirical mode decomposition," *IEEE Signal Processing Letters*, vol. 14, no. 12, pp. 936–939.
- [12] N. Rehman and D.P. Mandic, "Empirical mode decomposition for trivariate signals," *IEEE Transactions on Signal Processing*, vol. 58, no. 3, pp. 1059–1068, 2010.
- [13] N. Rehman and D.P. Mandic, "Multivariate empirical mode decomposition," *Proceedings of the Royal Society A*, vol. 466, no. 2117, pp. 1291–1302, 2010.
- [14] D.P. Mandic, N. Rehman, Z. Wu, and N.E. Huang, "Empirical mode decomposition based time-frequency analysis of multivariate signals," *IEEE Signal Processing Magazine*, vol. 30, no. 6, pp. 74–85, 2013.
- [15] S. Aviyente and A.Y. Mutlu, "Multivariate empirical mode decomposition for quantifying multivariate phase synchronization," *Eurasip Journal on Advances in Signal Processing*, 2011.
- [16] M.K.I. Molla, T. Tanaka, and T.M. Rutkowski, "Multivariate EMD based approach to EOG artifacts separation from EEG," *Proc. of IEEE International Conference on Acoustics, Speech and Signal Processing*, pp. 653–656, 2012.
- [17] E. Gallego-Jutgla, J. Sole-Casals, T.M. Rutkowski, and A. Cichocki, "Application of multivariate empirical mode decomposition for cleaning eye blinks artifacts from EEG signals," *Proc. of International Conference on Neural Computation Theory and Applications*, pp. 455–460, 2011.
- [18] I. Daubechies, J. Lu, and H.-T. Wu, "Synchrosqueezed wavelet transforms: An empirical mode decomposition-like tool," *Applied and Computational Harmonic Analysis*, vol. 30, pp. 243–261, 2011.
- [19] A. Ahrabian, D. Looney, L. Stankovic, and D.P. Mandic, "Synchrosqueezing-based time-frequency analysis of multivariate data," *Signal Processing*, vol. 106, pp. 331–341, 2015.
- [20] A. Ahrabian and D.P. Mandic, "A class of multivariate denoising algorithms based on synchrosqueezing," *Manuscript submitted for publication*.
- [21] A. Ahrabian, N. Rehman, and D.P. Mandic, "Bivariate empirical mode decomposition for unbalanced real-world signals," *IEEE Signal Processing Letters*, vol. 20, no. 3, pp. 245–248, 2013.
- [22] N. Rehman, M.W. Safdar, U. Rehman, and D.P. Mandic, "Dynamically-sampled bivariate empirical mode decomposition," *IEEE Signal Processing Letters*, vol. 21, no. 7, pp. 857–861, 2014.
- [23] N. Rehman and D.P. Mandic, "Filter bank property of multivariate empirical mode decomposition," *IEEE Transactions on Signal Processing*, vol. 59, no. 5, pp. 2421–2426, 2011.
- [24] S.J. Luck, *An introduction to the event-related potential technique*, The MIT Press, 2005.